Mon. Not. R. Astron. Soc. **000**, 1–9 (2043) Printed 4 September 2014 (MN LATEX style file v2.2)

The Effects of Orbital Inclination on the Scale Size and Evolution of Tidally Filling Star Clusters

Jeremy J. Webb[1], Alison Sills[1], William E. Harris[1], Jarrod R. Hurley[2] ⋆
[1] *Department of Physics and Astronomy, McMaster University, Hamilton ON L8S 4M1, Canada*
[2] *Centre for Astrophysics and Supercomputing, Swinburne University of Technology, P.O. Box 218, VIC 3122, Australia*

arXiv:1409.0879v1 [astro-ph.GA] 2 Sep 2014

4 September 2014

ABSTRACT
We have performed N-body simulations of tidally filling star clusters with a range of orbits in a Milky Way-like potential to study the effects of orbital inclination and eccentricity on their structure and evolution. At small galactocentric distances R_{gc}, a non-zero inclination results in increased mass loss rates. Tidal heating and disk shocking, the latter sometimes consisting of two shocking events as the cluster moves towards and away from the disk, help remove stars from the cluster. Clusters with inclined orbits at large R_{gc} have decreased mass loss rates than the non-inclined case, since the strength the disk potential decreases with R_{gc}. Clusters with inclined and eccentric orbits experience increased tidal heating due to a constantly changing potential, weaker disk shocks since passages occur at higher R_{gc}, and an additional tidal shock at perigalacticon. The effects of orbital inclination decrease with orbital eccentricity, as a highly eccentric cluster spends the majority of its lifetime at a large R_{gc}. The limiting radii of clusters with inclined orbits are best represented by the r_t of the cluster when at its maximum height above the disk, where the cluster spends the majority of its lifetime and the rate of change in r_t is a minimum. Conversely, the effective radius is independent of inclination in all cases.

Key words: galaxies: kinematics and dynamics globular clusters: general

1 INTRODUCTION

The gravitational dynamics of a three-body system which consists of a star orbiting in the combined potential of a star cluster and its host galaxy becomes increasingly complicated as one attempts to make the system more realistic. By treating all three members of the system (star, cluster, galaxy) as point masses, one can easily determine the tidal radius r_t (or Jacobi radius r_J) of the cluster, which is defined as the distance beyond which a star feels a stronger acceleration towards the host galaxy than the cluster itself (von Hoerner 1957). A straightforward derivation of r_t yields a function that depends on cluster mass M_{cl}, galaxy mass M_g, and the cluster's galactocentric distance R_{gc}:

$$r_t \simeq R_{gc}(\frac{M_{cl}}{2M_g})^{1/3} \quad (1)$$

Allowing the host galaxy to have a non-point-mass potential introduces significant complexity that has led to multiple analytic definitions of r_t (e.g. King 1962; Innanen, Harris, & Webbink 1983; Jordán et al. 2005; Binney & Tremaine 2008; Bertin & Varri 2008). However all analytic expressions of r_t, no matter how complex the tidal field, are limited by the assumptions that the host galaxy has a spherically symmetric potential and the cluster has a circular orbit. Under these assumptions the tidal field experienced by the cluster can be taken to be static. The derivation by Bertin & Varri (2008) is likely the most generalized derivation of r_t, as spherical symmetry is the only assumption it makes. In that work, r_t is defined as:

$$r_t = (\frac{GM_{cl}}{\Omega^2 \upsilon})^{1/3} \quad (2)$$

where Ω, κ and υ are:

$$\Omega^2 = (d\Phi_G(R)/dR)_{R_{gc}}/R_{gc} \quad (3)$$

$$\kappa^2 = 3\Omega^2 + (d^2\Phi_G(R)/dR^2)_{R_{gc}} \quad (4)$$

$$\upsilon = 4 - \kappa^2/\Omega^2 \quad (5)$$

Here Φ_G is the galactic potential, M and R_{gc} are the mass and galactocentric distance of the cluster respectively, Ω is

⋆ E-mail: webbjj@mcmaster.ca (JW)

its orbital frequency, κ is the epicyclic frequency of the cluster at R_{gc}, and υ is a positive dimensionless coefficient.

Since disk and triaxial elliptical galaxies have non-spherically symmetric potentials, and most Galactic globular clusters have non-circular orbits (Dinescu et al. 1999; Casetti-Dinescu et al. 2007, 2013), assuming that a cluster experiences a static tidal field as it evolves is clearly incorrect. Various works have studied the evolution of clusters in non-static tidal fields (Baumgardt & Makino 2003; Giersz & Heggie 2009, 2011; Renaud et al. 2011; Webb et al. 2013; Brockamp et al. 2014; Madrid et al. 2014), where the easiest approach is to first consider clusters with eccentric orbits in a spherically symmetric tidal field. These studies have shown that a cluster on an eccentric orbit will lose mass faster than if it has a circular orbit at apogalacticon R_a, but slower than if it has a circular orbit at perigalacticon R_p. The increased mass loss rate is attributed to tidal shocks during perigalactic passes and tidal heating.

Tidal heating and tidal shocks occur when a cluster experiences a time varying gravitational force. A tidal shock refers to a highly varying gravitational force experienced over a short period of time (e.g. perigalactic pass or passage through a disk). During a tidal shock, individual stars undergo an increase in energy that is dependent on their location within the cluster, and the cluster's binding energy is reduced. The orbits of stars during a shock can receive a significant kick, which can push loosely bound stars outside r_t (Gnedin & Ostriker 1997). Tidal heating on the other hand refers to a slowly varying gravitational force experienced over a long period of time (e.g. eccentric orbit or non-spherically symmetric potential). While the amount of energy injected into the cluster per unit time is much smaller than a tidal shock, over significant periods of time tidal heating can also have a strong influence on a cluster's evolution. Both mechanisms can provide stars with additional energy to escape the cluster that otherwise would remain bound, accelerating mass loss (Webb et al. 2013; Brockamp et al. 2014).

For a cluster on an eccentric orbit in a spherically symmetric potential, Equation 2 represents the instantaneous r_t of the cluster, which fluctuates between a maximum at R_a and minimum at R_p. In Webb et al. (2013) we demonstrate that the limiting radius r_L of a tidally filling cluster (the radius at which the stellar density approaches zero) traces r_t at all phases of its orbit. The agreement between r_L and r_t can be attributed to the cluster recapturing stars as it moves away from R_p, as well as energy injection from tidal shocks and tidal heating energizing bound stars to larger orbits within the cluster.

To better reflect the globular cluster population of disk galaxies, including the Milky Way, orbits need to be considered that are both eccentric and inclined to the plane of the disk. Studies of the effects of an inclined orbit on star clusters have primarily been focused on the effects of disk shocking as the cluster passes through the plane of the disk.

accelerate mass loss (Gnedin & Ostriker 1997; Gieles et al. 2007; D'Onghi et al. 2010; Madrid et al. 2014).

A cluster on an inclined orbit will not only undergo tidal shocks, but tidal heating as well even though its orbit is circular. If the cluster orbit is inclined *and* eccentric, which is the case for Galactic globular clusters, it will experience a third tidal shock at R_p. The overall effect on the mass loss rate and scale size of such a cluster has not been fully explored.

The purpose of this study is to both isolate and identify the effects of orbital inclination on the evolution of a star cluster and consider the combined effects of orbital inclination and eccentricity. Model N-body clusters with a range of orbital inclinations and eccentricities are evolved from t=0 to 12 Gyr in a Milky Way-like potential. In Section 2 we introduce the models and their initial conditions. In Section 3 we focus on how orbital inclination and eccentricity influence the evolution of cluster mass (M), r_t, velocity dispersion σ_V, r_L and half-mass radius r_m. We discuss the results of all our N-body models in Section 4. Specifically we suggest a method to correct both the dissolution time and the theoretical calculation of a cluster's scale size for inclination and/or eccentricity. We summarize our conclusions in Section 5.

2 THE MODELS

Model clusters are evolved from t=0 to 12 Gyr with the NBODY6 direct N-body code (Aarseth 2003). The initial mass of each model is $6 \times 10^4 M_\odot$ and has 96000 single stars and 4000 binaries. Stellar masses are drawn from a Kroupa, Tout, & Gilmore (1993) initial mass function between $0.1M_\odot$ and $30M_\odot$, with each star assigned a metallicity of $Z = 0.001$. The distribution of stellar positions and velocities follow a Plummer density profile with a cutoff at $10r_m$ (Plummer 1911; Aarseth et al. 1974). The initial half mass radius of each model is set to 6 pc, which ensures that all models exhibit bound stars at or beyond r_t and can be considered tidally filling.

To first study the effects of orbital inclination on star clusters, we simulate model clusters with circular orbits at 6 kpc and 18 kpc that have orbital inclinations of 0°, 22°, and 44°. We then study the combined effects of orbital eccentricity and inclination by simulating a cluster with an orbital eccentricity of 0.5, orbiting between R_p of 6 kpc and R_a of 18 kpc, with the same orbital inclinations. We selected these orbital parameters to allow us to compare a cluster with an eccentric orbit to clusters with circular orbits at R_p and R_a over a range of inclinations. The models with orbital inclinations of 0° were first introduced in Webb et al. (2014), hence we refer the reader to that study for additional details on the input parameters used in our models.

The clusters orbit within a Milky Way-like potential made up of a $1.5 \times 10^{10} M_\odot$ point mass bulge (Equation 6), a Miyamoto & Nagai (1975) disk (Equation 7 with $M_d = 5 \times 10^{10} M_\odot$, a= 4.5 kpc, and b = 0.5 kpc), and a logarithmic halo potential (Equation 8 (Xue et al. 2008)). The halo is scaled such that the three potentials combine to give a circular velocity (v_C) of 220 km/s at a galactocentric distance of 8.5 kpc in the plane of the disk (Aarseth 2003). Therefore R_C in Equation 8 is 8.8 kpc. The initial radius in the plane of the disk (R_{xy}), initial height above disk (Z_i), R_p, eccentricity and orbital inclination of each cluster is given in Table 1. Note that model names are based on orbital eccentricity (e.g. e05), circular orbit distance or apogalactic distance (e.g. r18) and orbital inclination (e.g. i22).

Table 1. Model Input Parameters

Model Name	R_{xy} kpc	Z_i kpc	R_p kpc	e	i degrees
e0r6i0	6	0	6	0	0
e0r6i22	5.56	2.25	6	0	22
e0r6i44	4.32	4.17	6	0	44
e05r18i0	6	0	6	0.5	0
e05r18i22	5.56	2.25	6	0.5	22
e05r18i44	4.32	4.17	6	0.5	44
e0r18i0	18	0	18	0	0
e0r18i22	16.69	6.74	18	0	22
e0r18i44	12.73	12.73	18	0	44

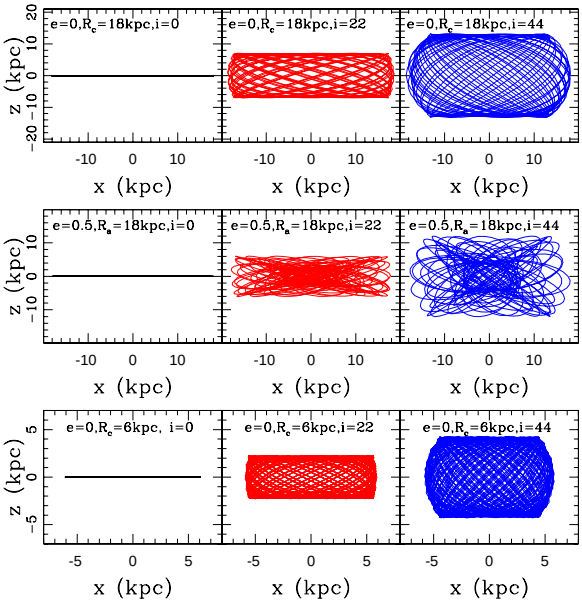

Figure 1. Orbits of all model clusters. Clusters with circular orbits at 6 kpc are in the lower row, with orbital eccentricities of 0.5 and perigalactic distances of 6 kpc in the middle row, and circular orbits at 18 kpc in the top row. Orbital inclination changes from 0° in the left column, to 22° in the middle column, to 44° in the right column.

$$\Phi_{bulge}(R_{gc}) = \frac{-GM_b}{R)gc} \tag{6}$$

$$\Phi_{disk}(R_{xy}, z) = \frac{-GM_d}{\sqrt{R_{xy}^2 + [a + \sqrt{b^2 + z^2}]^2}} \tag{7}$$

$$\Phi_{halo}(R_{gc}) = \frac{1}{2}(v_C^2)LOG(R_{gc}^2.0 + R_C^2.0) \tag{8}$$

In order to better visualize the orbits of each model cluster, specifically how they evolve with time, we have plotted the x and z coordinates at each time step for each cluster in Figure 1. The orbital eccentricity, circular orbit distance or apogalactic distance, and orbital inclination are marked in each panel.

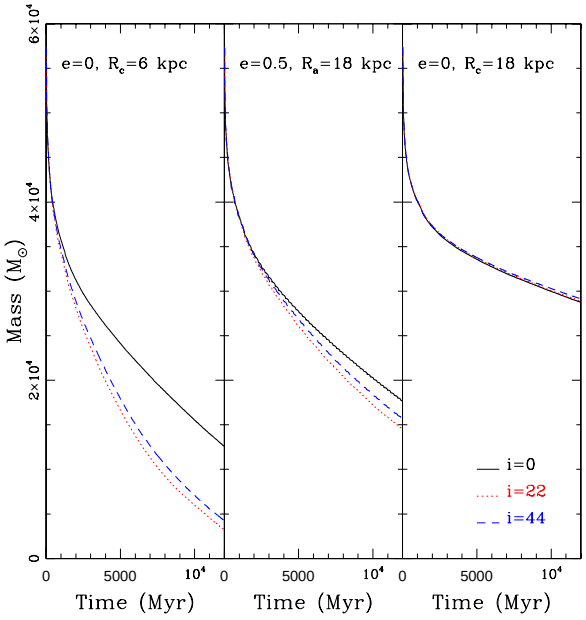

Figure 2. The evolution of total cluster mass over time for clusters with a circular orbit at 6 kpc (left panel), an orbital eccentricity of 0.5 and an apogalactic distance of 18 kpc (center panel) and a circular orbit at 18 kpc (right panel). The black solid lines, red dotted lines, and blue dashed lines correspond to models with orbital inclinations of 0°, 22°, and 44° respectively.

3 INFLUENCE OF ORBITAL INCLINATION

To study the effects of orbital inclination on the scale sizes of clusters, we focus on the evolution of the mass, tidal radius, velocity dispersion, limiting radius and half-mass radius of all bound stars in each model cluster. A star is considered to be bound if the difference between its kinetic energy and the potential energy due to all other stars in the simulation is less than 0.

3.1 Mass

The total bound mass of each cluster is plotted in Figure 2 as a function of time. For any cluster, mass loss is driven by stellar evolution and the tidal stripping of stars pushed beyond r_t. For clusters with circular orbits in the plane of the disk, the mean mass loss rate increases with decreasing R_{gc} due to the increased strength of the tidal field. For clusters which experience non-static tidal fields (those with eccentric and/or inclined orbits) tidal heating and tidal shocks due to a sudden increase in the local gravitational potential (passage through a galactic disk or near R_p) are additional sources of mass loss. For example, clusters with circular orbits at 6 kpc that are inclined lose mass at a higher rate than the $i = 0$ case, with e0r6i22 losing mass the fastest.

Model e0r6i22 (22° inclination) loses more mass than e0r6i44 (44° inclination) over 12 Gyr for two reasons. First, e0r6i22 passes through the disk more often, thus experiencing more frequent disk shocking. Secondly, the tidal field of the disk is proportional to z^{-1} for a given R_{xy} (see Equation 7, so the cluster e0r6i22 spends the majority of its time in a stronger tidal field. e0r6i44 is far enough from the plane

of the disk that when at its maximum height z_{max} it experiences a weaker and nearly spherically symmetric tidal field such that tidal heating is less of a contributing factor. Model clusters with higher inclinations, like those performed by Madrid et al. (2014), are also in agreement with our findings. Clusters with extremely high inclinations not only pass through the disk more frequently due to shorter orbital periods, but also pass through the disk perpendicular to the Galactic plane. Crossing the disk at such a high inclination increases the amount of energy imparted to cluster stars. Stronger and more frequent disk shocks experienced by high inclination clusters result in an accelerated mass loss rate compared to the models presented here.

For circular orbits at 18 kpc, there is very little difference between the mass profiles of the inclined and non-inclined cases. The strength of a Miyamoto & Nagai (1975) disk decreases as R_{xy}^{-1} (Equation 7). Hence for clusters orbiting at similarly large distances, the majority of the disk's mass is within their orbit, and the clusters evolve more as if they are in a spherically symmetric potential. However it is surprising that the clusters on inclined orbits are actually more massive at all times than the $i = 0$ case since we expect these clusters to undergo some degree of disk shocking and tidal heating. This will be addressed in Section 4.2.

For clusters with eccentric orbits, periodic episodes of enhanced mass loss due to perigalactic passes are present in all three cases. In the case of a cluster with orbital eccentricity e in the plane of the disk (e05r180), the cluster takes (1+e) times longer to reach dissolution than a cluster with a circular orbit at R_p, or (1-e) times shorter than a cluster with a circular orbit at R_a. The dissolution time scaling is in agreement with Baumgardt & Makino (2003), who defines the dissolution time as the time it takes for the cluster to reach $100 M_{\odot}$. Given that the behaviour of collisional N-body simulations can become noisy at late times when only a small number of stars remain, we have checked the results of Figure 2 against an alternative definition of the dissolution time (when the cluster reaches 10% of its original mass) and find no noticeable change.

The amount of mass lost during a perigalactic pass decreases with increasing inclination because the tidal field is weaker at R_p when the cluster is above or below the plane of the disk. However, the inclined and eccentric clusters still lose more mass than e05r18i0 because they undergo additional mass loss via disk shocking and increased tidal heating. While tidal heating has been shown to be a factor for clusters with eccentric orbits in the plane of the disk (Webb et al. 2013), it is even more effective for clusters with inclined orbits as the rate of change of the local potential is higher. The rate of change of the local potential is reflected in plots of r_t versus time and the cluster's height above the disk as discussed in Sections 3.2 and 4.1 respectively. Disk shocking, while still an additional source of mass loss, is less effective than if the cluster had a circular orbit at R_p because disk passages occur at larger galactocentric radii. The combined effects result in the (1-e) scaling factor from the perigalactic case remaining an accurate indicator of dissolution time (within 9%) for a given orbital inclination, while the R_a case does not (greater than 30%).

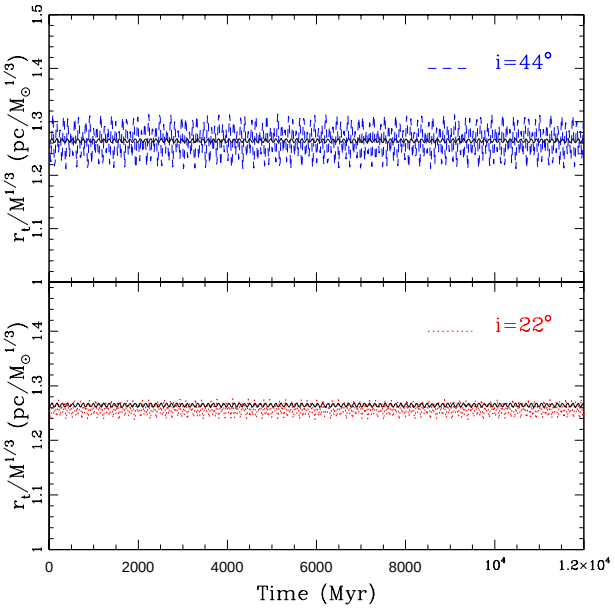

Figure 3. The evolution of the mass normalized tidal radius over time for clusters with a circular orbit at 6 kpc. The black solid lines, red dotted lines, and blue dashed lines correspond to models with orbital inclinations of 0°, 22°, and 44° respectively.

3.2 Tidal Radii

Tidal shocks and tidal heating can be traced by the evolution of r_t over the course of a cluster's orbit and lifetime. Any correlation between r_t and orbital phase indicates that tidal heating is occurring, while a tidal shock occurs when r_t suddenly goes from decreasing to increasing. To illustrate events of tidal shocking and heating, we plot the instantaneous r_t of the models with circular orbits at 6 kpc in Figure 3. Model e0r6i22 is plotted in the lower panel (red) and e0r6i44 in the upper panel (blue). The non-inclined case, e0r6, has been plotted in black in both panels. The instantaneous r_t has been calculated via Equation 2 given each cluster's mass and instantaneous location in the Galactic potential. To remove any dependence of r_t on the mass loss rate and focus on effects due to cluster orbit, r_t has been normalized by $M^{\frac{1}{3}}$ (See Equation 1). Hence for clusters with circular orbits in the plane of the disk, their mass normalized r_t never changes.

Figure 3 indicates that the r_t of clusters with inclined orbits fluctuates by ±5% over the course of a single inclined orbit. The fluctuations in r_t can be understood by plotting the mass normalized r_t at all locations in the Galactic potential with $R_{xy} < 20$ kpc and $|z| < 20$ kpc in Figure 4. A cluster will have its largest r_t when at its maximum height above the disk, with r_t decreasing as the cluster approaches the disk. The process is then reversed as the cluster leaves the disk again on its way to its maximum distance below the disk.

For clusters orbiting at 18 kpc we see that the tidal field is essentially spherically symmetric. The tidal field imposed by the Galactic disk alone, and its gradient, become independent of z at approximately 15 kpc. Therefore a possible cut-off radius for the influence of orbital inclination may ex-

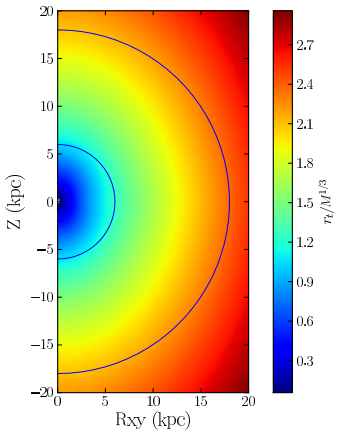

Figure 4. The mass normalized instantaneous tidal radius at all points in the $R_{xy} - z$ plane. Solid lines mark galactocentric distances of 6 kpc and 18 kpc.

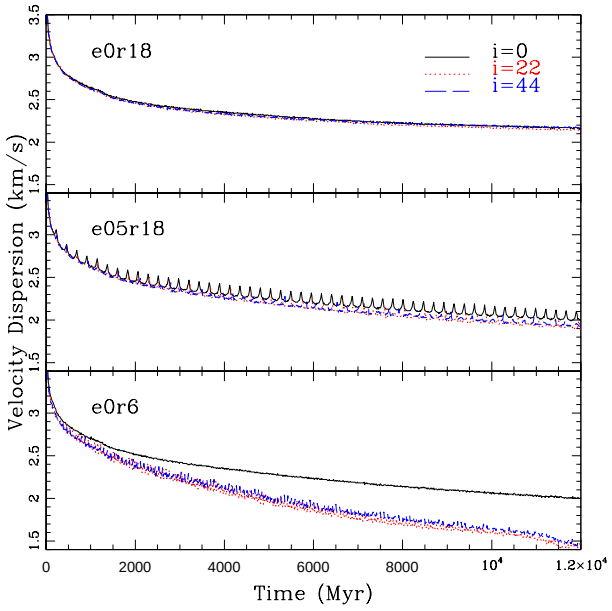

Figure 5. The evolution of the velocity dispersion of all bound stars over time for clusters with a circular orbit at 6 kpc (bottom panel), an orbital eccentricity of 0.5 and an apogalactic distance of 18 kpc (center panel) and a circular orbit at 18 kpc (top panel). The black solid lines, red dotted lines, and blue dashed lines correspond to models with orbital inclinations of 0°, 22°, and 44° respectively.

ist. Future studies on how this cut-off radius may depend on initial cluster conditions or the assumed structure of the Galactic disk are planned.

For a cluster on an inclined *and* eccentric orbit, r_t will also be growing and shrinking as it moves towards and away from R_p. With the distance above or below the disk at R_p and R_a changing from one orbit to the next, a cluster with such a complicated orbit cannot be considered to be in any form of equilibrium, but is instead in a constant state of flux.

3.3 Velocity Dispersion

The clearest demonstration of how these model clusters are affected by tidal shocks and tidal heating is in the evolution of the global three dimensional velocity dispersion σ_V of all bound stars in Figure 5. The general trend in all cases is for σ_V to decrease with time as mass segregated low-mass stars with higher velocities escape and the cluster loses mass. For a cluster on a circular orbit in the plane of the disk, the decrease in σ_V is smooth. Periodic spikes in σ_V, that are only present in the inclined and eccentric clusters, are points where a sudden injection of energy (a tidal shock) has occurred. A sudden increase in energy can cause a significant increase in stellar velocities (Webb et al. 2014).

For models on circular inclined orbits, each peak in σ_V signifies a disk shock. The peak is followed by a sharp decrease in σ_V as r_t decreases and stars with lower binding energies (and high velocities) escape. σ_V then slowly increases due to both the recapturing of temporarily unbound stars as r_t begins to re-expand, and tidal heating as the cluster moves through a non-static tidal field. Hence the cluster expands as it moves towards z_{max}. The process then repeats itself when the clusters moves through the disk during the second half of its orbit. The strength of the shock decreases with R_{gc} as the disk's contribution to the Galactic potential decreases.

The situation is slightly more complicated for models with eccentric *and* inclined orbits like e05r18i22 and e05r18i44 . The cluster still crosses the disk twice per orbit, but since the orbit is non-circular the disk passages occur at different galactocentric radii. The disk shock that occurs nearest R_p will be much stronger than the shock occurring near R_a. The weaker second shock results in the mass loss rate of inclined and eccentric clusters being only marginally higher than the non-inclined case. It is also important to note that when a cluster has a circular and inclined orbit, tidal heating and the recapturing of unbound stars is able to increase σ_V between shocks. But when the cluster has an eccentric and inclined orbit, the weaker tidal field experienced as the cluster moves towards R_a only injects enough energy to keep σ_V constant between shocks. Therefore clusters on eccentric and inclined orbits do not expand in size as efficiently as clusters on inclined and circular orbits near R_p while the cluster moves towards z_{max}.

3.4 Limiting Radii

We next consider the effect of inclination on the [limiting radius]. For the purposes of this study, the limiting radius is defined as the average cluster-centric distance of all bound stars located beyond the instantaneous r_t (Webb et al. 2013). The interplay between a changing theoretical r_t and the actual size of the cluster r_L is illustrated in Figure 6 where we plot the ratio of $\frac{r_L}{r_t}$ as a function of time. Based on our definition of r_L, the ratio will always be slightly larger than 1.0.

How a cluster responds to its instantaneous r_t is indicated by how much the ratio fluctuates around its mean value. For example, it has been shown that clusters which orbit in the plane of the disk fill their instantaneous r_t at all

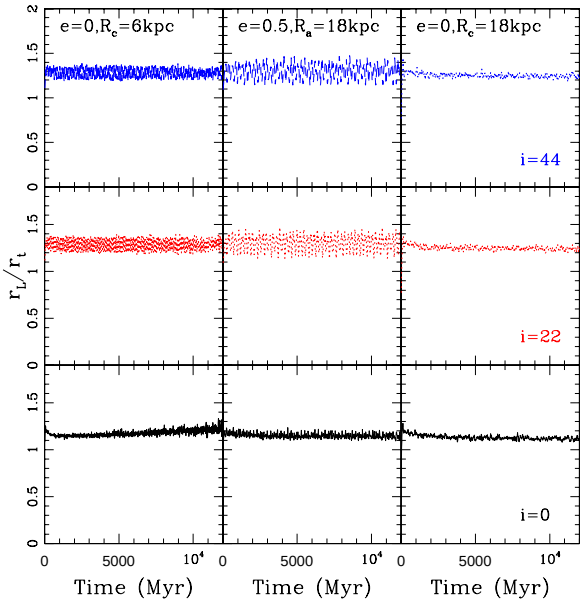

Figure 6. The ratio of the limiting radius of each cluster to its tidal radius as a function of time for clusters with a circular orbit at 6 kpc (left panels), an orbital eccentricity of 0.5 and an apogalactic distance of 18 kpc (center panels) and a circular orbit at 18 kpc (right panels). The black (bottom panels), red (middle panels), and blue (top panels) lines correspond to models with orbital inclinations of 0°, 22°, and 44° respectively.

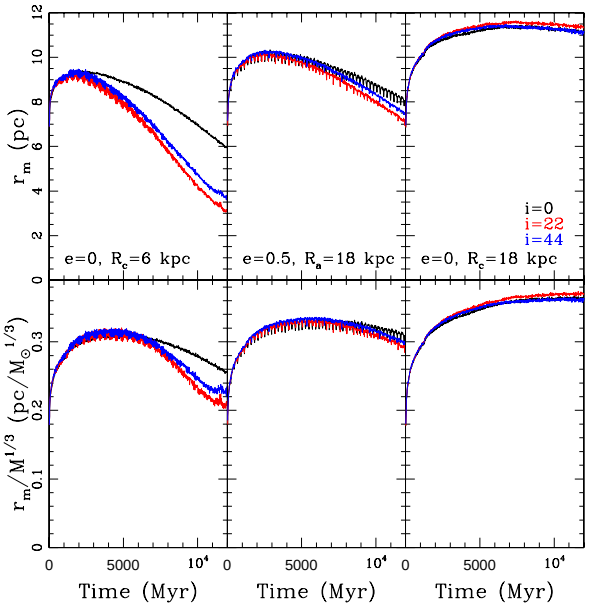

Figure 7. The evolution of the half mass radius (top panels) and the half mass radius normalized by mass (bottom pannels) over time for clusters with a circular orbit at 6 kpc (left panels), an orbital eccentricity of 0.5 and an apogalactic distance of 18 kpc (center panels) and a circular orbit at 18 kpc (right panels). The black solid lines, red dotted lines, and blue dashed lines correspond to models with orbital inclinations of 0°, 22°, and 44° respectively.

times (Webb et al. 2013), which is why the ratio is nearly constant as a function of time for the non-inclined cases. The inclined cases, however all fluctuate around the mean $\frac{r_L}{r_t}$ value of the non-inclined case. The fluctuations are not the result of a non-static field, as e05r18 has a nearly constant ratio despite orbiting between 6 kpc and 18 kpc in the plane of the disk. The oscillations are due to inclined clusters being subject to increased tidal heating and additional shocking events per orbit compared to clusters in the plane of the disk. Before the cluster even has a chance to respond to its new local potential, which takes approximately one crossing time (Madrid et al. 2014), the local potential has already changed so quickly that the cluster never comes to equilibrium.

During each orbit, when the cluster is moving away from the disk and towards z_{max} it will be slightly underfilling as r_t expands. As the cluster approaches z_{max} it slows down and therefore has time to respond to its local potential and fill r_t. As the cluster moves away from z_{max} and towards the plane of the disk, the cluster is slightly overfilling since r_t is now decreasing. As the cluster passes through the plane of the disk and undergoes a disk shock, outer stars can become permanently or temporarily unbound, and the cluster becomes briefly tidally filling before r_t begins to increase again.

3.5 Half-mass Radius

The inner structure of globular clusters, observationally traced by the effective radius r_h, is far more robust and less model dependent than r_L (e.g. McLaughlin & van der Marel 2005; Webb, Sills, & Harris 2012; Puzia et al. 2014). For N-body simulations, the half-mass radius r_m is more commonly used to probe the inner regions of globular clusters (e.g. Gieles et al. 2010; Madrid et al. 2012; Webb et al. 2013). The three-dimensional half mass radius is taken to be the radius enclosing half of the total bound mass, including both bound objects orbiting beyond r_t and stellar remnants. The latter points resulting in r_m being on average slightly larger than r_h.

The half-mass radius and the mass normalized half-mass radius of each cluster as a function of time are plotted in Figure 7. It should be noted that our clusters all have final half-mass radii 2-3 times greater than most actual globular clusters. Future studies will explore the influence of inclined orbits in disk potentials on a wider range of initial r_m.

Figure 7 suggests that the inner structure of a star cluster is less affected by changes in orbital inclination than r_L. If we first consider the models orbiting at 6 kpc, the inclined clusters are smaller because they lose mass at a faster rate than the non-inclined case. However if we normalize by mass, the mass normalized r_m of all three cases are nearly identical for almost 7 Gyr. At 7 Gyr, the inclined clusters are approximately $1 \times 10^4 M_\odot$ in mass, and are in the process of dissolving. The eccentric clusters only differ in r_m by 1 pc after 12 Gyr and the clusters orbiting at 18 kpc differ by less than 0.5 pc. After normalizing by cluster mass, the eccentric and 18 kpc clusters are nearly always identical in size.

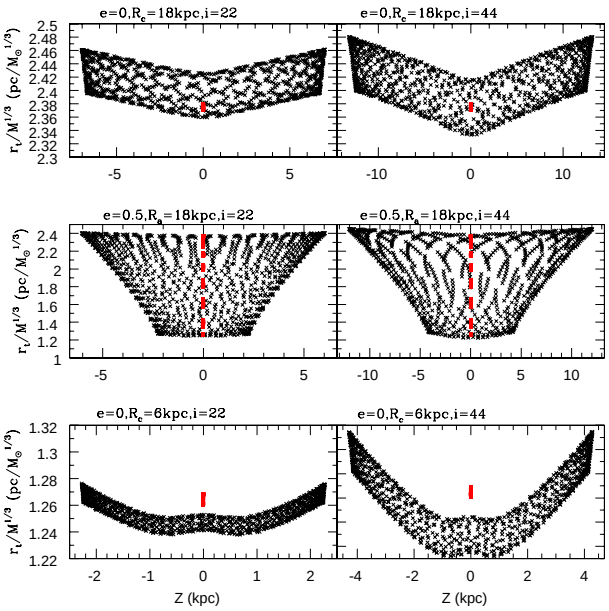

Figure 8. Mass normalized tidal radius as a function of height above the disk z for all inclined model clusters (black crosses). Data points are equally spaced in time and cover 12 Gyrs of evolution, so the density of points reflects the amount of time the cluster spends at a given z. Red squares mark model clusters with orbits in the plane of the disk.

4 DISCUSSION

Our simulations indicate that the primary effect of an inclined orbit in a non-spherically symmetric potential is an increased mass loss rate due to tidal heating and shocking. To apply these findings to observations of star clusters, we need to know how tidal shocks and heating depend on cluster orbit and how they would influence the calculated size of a cluster.

4.1 Tidal Heating and Shocks

The increased mass loss rate experienced by clusters on inclined orbits is a direct result of them being subject to both tidal heating and tidal shocks, neither of which clusters on non-inclined circular orbits experience. We examine both of these effects further by plotting the mass normalized r_t of each model cluster as a function of its height z over 12 Gyrs (Figure 8). Since data points are equally spaced in time, the density of points reflects the proportion of its lifetime a cluster spends at a given z.

In Figure 8, episodes of tidal heating are indicated by gradual changes in r_t. All model clusters experience some degree of tidal heating as r_t decreases while the cluster moves inward from z_{max}. Tidal shocks are seen in Figure 8 when the mass normalized r_t goes from decreasing to increasing. For an inclined orbit that is perfectly circular (e=0), a disk shock would be a singular event as r_t reaches a minimum at $z = 0$. However, since the orbits of our model clusters at 6 kpc and 18 kpc are not perfectly circular ($e \leqslant 0.05$), the situation is slightly more complicated. At smaller R_{xy} (6 kpc) the *disk shock* appears to consist of two shocking events, just before and just after the cluster passes through the plane of the disk, unless the disk passage actually occurs at R_p. The increase in r_t to a local maximum between the shocks lets the cluster temporarily expand freely. The dual shocks are what separates a disk shocking event from a more simple tidal shock, like a perigalactic pass, and make it more efficient at removing stars from the cluster. However, since the shape of the disk potential changes and strength of the disk decreases with R_{xy}, both shocks are not necessarily equal in magnitude, with one of the shocks sometimes being weaker and even negligible when orbits are near circular. At larger R_{xy} (18 kpc), the decreased strength of the disk results in the disk shock being a singular event. Inclined *and* truly eccentric clusters (middle row of Figure 8) experience a strong dual tidal shock during its innermost disk passage, a weaker single shock during its outermost disk passage, and a third shock during each perigalactic pass.

Figure 8 indicates that inclined, eccentric clusters experience varying amounts of tidal heating from one orbit to another. While some orbits keep the cluster at a high z until just before crossing the disk (minimizing tidal heating), other orbits gradually bring the cluster in from z_{max} to z=0 (maximizing tidal heating). The complex orbits of clusters that are inclined and eccentric makes quantifying the effects of tidal heating or shocking difficult. However this study suggests that the evolution of a cluster with an eccentric and inclined orbit is more similar to a cluster with the same eccentricity and $i = 0°$ rather than a cluster with the same i orbiting at R_p with e=0.

4.2 The Effective Tidal Radius of an Inclined Orbit

Because of the chaotic evolution of the instantaneous r_t of a cluster with an inclined orbit, and because r_L does not precisely trace r_t as in a spherically symmetric potential, it is difficult to define what exactly the *size* of a star cluster is. While an inclined cluster may appear to have an r_L greater than its current r_t, this could simply be a function of its current orbital phase and not accurately indicate its current dynamical state. As we saw in Figure 6, an inclined cluster ranges between being tidally over-filling and under-filling, except at z_{max} and $z = 0$ when r_L and r_t are near equal.

We wish to define an *effective* r_t for a cluster with an inclined orbit, in order to get a sense of its dynamical state and whether or not the cluster is tidally filling. When defining an *effective* r_t, it should ideally represent a stable state during the cluster's orbit at which the cluster spends the majority of its orbit. We consider the rate of change in the mass normalized tidal radius as a function of height above the disk in Figure 9. The r_t of a cluster near the plane of the disk fluctuates dramatically during the disk passage, and only represents a brief portion of the total orbit. Setting the *effective* r_t equal to the r_t near $z = 0$ would be equivalent to setting the r_t of a cluster on an eccentric orbit equal to its r_t at R_p, which we know to be incorrect (Webb et al. 2013). The clear choice is to let the *effective* r_t of a cluster with an inclined orbit be equal to its instantaneous r_t at z_{max}. Not only is the rate of change in r_t is at its minimum when the cluster is both approaching and leaving z_{max}, but inclined clusters also spend the majority of their lifetime near

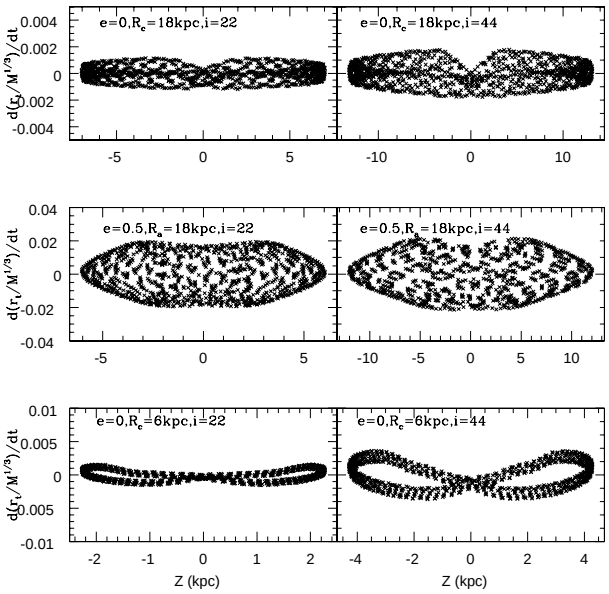

Figure 9. The rate of change in the mass normalized tidal radius ($pc/M_{\odot}s^{-1}$ as a function of height above the disk z for all inclined model clusters. Data points are equally spaced in time and cover 12 Gyrs of evolution, so the density of points reflects the amount of time the cluster spends at a given z.

z_{max}. Therefore the time averaged r_t of each model also corresponds to r_t at z_{max}.

5 SUMMARY

In this paper, we simulated the evolution of star clusters orbiting in a Milky Way-like potential with a range of orbital inclinations in order to study the effects of orbital inclination on their dynamical and structural evolution. The main factors which separate star clusters on inclined orbits are tidal heating and tidal shocking. While clusters on eccentric orbits in a spherically symmetric potential do experience tidal heating and tidal shocking at perigalacticon, both inclination and eccentricity are more dominant when the orbit is inclined and a galactic disk is present. The strength of both tidal heating and shocking due to an inclined orbit however weakens with R_{gc}. By 18 kpc, the Galactic potential is nearly spherically symmetric and orbit inclination is nearly negligible. When performing N-body simulations of remote halo clusters, such as Pal 4 and Pal 14 (Zonoozi et al. 2011, 2014), unless their orbits are highly eccentric and bring them deep into the inner regions of the Milky Way it can be safely assumed that they orbit in a spherically symmetric potential.

We have simulated model clusters with identical initial conditions with both circular and eccentric orbits over a range of orbital inclinations to determine the main effects of tidal heating and tidal shocking. Our main conclusions are as follows:

- For clusters with small R_{gc}, inclined clusters experience an enhanced mass loss rate due to increased tidal heating and two tidal shocking events during a disk passage. Clusters with small orbital inclinations are more strongly affected since they spend a longer time in the stronger disk potential.
- At higher R_{gc}, the strength of the galactic disk is weaker, minimizing the effects of tidal heating and disk shocking. Furthermore, r_t at z_{max} is larger than in the plane of the disk, so inclined clusters will actually lose mass at a lower rate than non-inclined clusters.
- Disk shocking causes a temporary increase in σ_V, followed by a sharp drop as stars that have been energized to higher velocities escape the cluster.
- Between shocking events, σ_V can remain constant or even increase due to tidal heating.
- The local potential around a cluster with an inclined orbit is in a constant state of flux, so an inclined cluster is not able respond to its instantaneous r_t except at z_{max}. The r_L of the cluster instead fluctuates around r_t at z_{max}, ranging between being tidally under-filling and over-filling as it travels away from or towards the disk respectively.
- Tidal heating and shocking have a negligible effect on the inner region of the cluster ($r < r_m$).
- The tidal radius of a cluster on an inclined (or inclined and eccentric) orbit is best approximated by assuming it has a circular orbit at its maximum height above the disk: $r_t(R_{xy}, z, e, i) = r_t(R_{xy}, z_{max})_{z_{max}}$

The final point that r_m is unaffected by orbital inclination is helpful when studying globular clusters in other galaxies. More specifically in disk galaxies or elliptical galaxies that are triaxial, the commonly observed effected radius is independent of the orientation of the clusters orbit in the galactic potential, which would be difficult to determine. Therefore the effective radius is solely dependent on the cluster's three dimensional position and orbital eccentricity.

The combined effects of orbital inclination and eccentricity on a cluster are complex. The cluster experiences a strong disk shock when it crosses the disk near R_p, a weak disk shock when crossing near R_a, and a tidal shock during its perigalactic pass. Furthermore, the cluster does not cross the disk at the same R_{gc} or reach R_p at the same z from one orbit to the next. The cluster is also constantly subjected to tidal heating since both the R_{gc} and z coordinate of the cluster change with time. Ultimately, predicting the evolution of a cluster with an inclined and eccentric orbit is difficult, although the effects of orbital inclination clearly decrease with increasing orbital eccentricity since high-e clusters spend the majority of their lifetime at large galactocentric radii. We do find that the dissolution time of such a cluster can be approximated to be (1+e) times longer than the dissolution time of a cluster with a circular orbit at R_p and the same orbital inclination, in agreement with the work of Baumgardt & Makino (2003) for clusters with non-inclined obits.

Exploring a large parameter space in both orbital inclination and eccentricity, and their subsequent effects on clusters, is necessary as the orbits of Galactic globular clusters are neither circular nor in the plane of the disk. As previously mentioned, we also wish to explore how the initial r_m of a cluster changes its dynamical evolution in a non-spherically symmetric potential. The ultimate goal is to be able to predict the size of any cluster no matter its position or orbit in an arbitrary tidal field. Any clusters whose theoretical and observational sizes do not match may indicate

recently captured clusters that have not spent long in their current tidal field. When theory and observations do match, we will be able to predict other dynamical properties of a cluster, including its stellar mass function, and rewind the cluster's dynamical clock to determine its initial mass and initial size.

6 ACKNOWLEDGEMENTS

JW, WEH and AS acknowledge financial support through research grants and scholarships from the Natural Sciences and Engineering Research Council of Canada. This work was made possible by the facilities of the Shared Hierarchical Academic Research Computing Network (SHARCNET:www.sharcnet.ca) and Compute/Calcul Canada.

REFERENCES

Aarseth, S.J. 2003, Gravitational *N*-body Simulations: Tools and Algorithms (Cambridge Monographs on Mathematical Physics). Cambridge University Press, Cambridge
Aarseth, S., Hénon, M., Wielen, R., 1974, A&A, 37, 183
Baumgardt H., Makino J. 2003, MNRAS, 340, 227
Bertin, G. & Varri, A. L. 2008, ApJ, 689, 1005
Binney, J. & Tremaine, S. 2008, Galactic dynamics second edition (Princeton, NJ, Princeton University Press, 1987, 747 p.)
Brockamp, M., Küpper, A. H. W, Ties, I., Baumgardt, H., Kroupa, P, 2014, MNRAS, 441, 150
Casetti-Dinescu, D.I., Girard, T.M., Herrera, D., van Altena, W.E., López, C.E., Castillo, D.J. 2007, AJ, 134, 195
Casetti-Dinescu, D.I., Girard, T.M., Jíková, L., van Altena, W.F., Podestá, F., López, C.E. 2013, AJ, 146, 33
D'Onghia, E., Springel, V., Hernsquist, L., & Keres, D. 2010, ApJ, 709, 1138
Dinescu, D.I., Girard, T.M., van Altena, W.E. 1999, AJ, 117, 1792
Gieles, M., Athanassoula, E., Portegies Zwart, S. F., 2007, MNRAS, 376, 809
Gieles, M., Baumgardt, H., Heggie , D. C., Lamers, H.J.G.L.M. 2010, MNRAS, 408, L16
Giersz, M. & Heggie, D. C. 2009, MNRAS, 395, 1173
Giersz, M. & Heggie, D. C. 2011, MNRAS, 410, 2698
Gnedin, O.Y. & Ostriker, J.P. 1997, ApJ, 474, 223
Henon M. 1961, Annales d'Astrophysique, 24, 369
Innanen, K. A., Harris, W.E., Webbink, R.F. 1983, AJ, 88, 338
Johnston, K.V., Spergel, D.N., Hernquist, L. 1995, ApJ, 451, 598
Jórdan, A., Côté, P., Blakeslee, J. P., Ferrarese, L., McLaughlin, D. E. , Mei, S., Peng, E. W., Tonry, J. L., Merrit, D., Milosavljević, M., Sarazin, C. L., Sivakoff, G. R., West, M. J., 2005, ApJ, 634, 1002
King, I. R. 1962, AJ, 67, 471
Kroupa, P., Tout C.A., Gilmore, G. 1993, MNRAS, 262, 545
Leigh, N., Giersz, M., Webb, J.J., Hypki, A., de Marchi, G., Kroupa, P., Sills, A. 2013, MNRAS, 436, 3399
Madrid, J.P., Hurley, J.R., Sippel, A.C., 2012, ApJ, 756, 167
Madrid, J.P., Hurley, J.R., Martig, M., 2014, ApJ, 784, 95
McLaughlin, D. E. & van der Marel, R. P. 2005, ApJs, 161, 304
Miyamoto, M. & Nagai, R. 1975, PASJ, 27, 533
Plummer, H.C. 1911, MNRAS, 71, 460
Praagman, A., Hurley, J., Power C. 2010, New Astron., 15, 46
Puzia, T.H., Paolillo, M., Goudfrooij, P., Maccarone, T.J., Fabbiano, G., Angelini, L. 2014, ApJ, 786, 78
Renaud, F., Gieles, M., Christian, M. 2011, MNRAS, 418, 759
von Hoerner, S. 1957, ApJ, 125, 451
Webb, J. J., Sills, A., Harris, W.E. 2012, ApJ, 746, 93
Webb, J.J., Harris, W.E., Sills, A., Hurley, J.R. 2013, ApJ, 764, 124
Webb, J.J., Leigh, N., Sills, A., Harris, W.E., Hurley, J.R. 2014, MNRAS, 442, 1569
Xue, X.X. et al., 2008, ApJ, 684, 1143
Zonoozi, A. H., Küpper, A. H. W, Baumgardt, H., Haghi, H., Kroupa, P., Hilker, M. 2011, MNRAS, 411, 1989
Zonoozi, A. H., Haghi, H., Küpper, A. H. W, Baumgardt, H., Frank, M.J., Kroupa, P 2014, MNRAS, 440, 3172

This paper has been typeset from a TEX/ LATEX file prepared by the author.